Proceedings of the
International Conference on Mechanical Engineering 2011
(ICME2011) 18- 20 December 2011, Dhaka, Bangladesh

ICME11-TH-004

.

CFD MODELLING OF AIR-FIRED AND OXY-FUEL COMBUSTION IN A 100 KW UNIT FIRING PROPANE

Audai Hussein Al-Abbas and Jamal Naser

Faculty of Engineering and Industrial Science, Swinburne University of Technology, Australia.

ABSTRACT

A computational fluid dynamics (CFD) modelling study is undertaken integrating the air-fired and oxy-fuel combustion cases for chemical reactions, radiative heat transfer, and gas compositions into a 3-D hybrid unstructured grid CFD code. A swirl injection system is used to achieve the flame stability of the turbulent non-premixed combustible gases. An Eddy Breakup (EBU) combustion model with appropriate empirical coefficients is employed for this study. Validation and comparison of both combustion cases with the experimental data, which conducted on a 100 kW facility unit, were made by comparing the temperature distribution levels and species concentration levels. The oxy-fuel combustion case showed that the flame is obviously concentrated in the central region, and it is not spread inside the furnace compared to the air-fired flame. The swirl effect is certainly used to enhance the turbulent mixing and to achieve the internal recirculation of flames. By switching to oxy-fuel fired combustion, results show that the carbon dioxide concentration increases from around 15 % (kg/kg) to 76 % (kg/kg) under wet basis in flue gas. Under the same operating conditions, combustion delay is clearly observed in oxy-fuel combustion case compared to air-fired case due to incomplete consumption of oxygen at the near-burner region. This CFD model, after validation against experimental data, is expected to provide a strong confidence on the combustion characteristics of both combustion cases, particularly at the challenging locations of the furnace.

Keywords: Non-Premixed Flames, Oxy-Fuel Combustion, CO_2 Capture, Swirl Effect, and CFD.

1. INTRODUCTION

Over the past years, environmental concerns about anthropogenic emissions of greenhouse gases (GHG) are significantly leading to global climate change [1]. The most important resource of these anthropogenic GHG emissions is carbon dioxide emission. Recently, fossil fuels are still providing around 85% of the world's demand of electrical energy [2]. The most effective technique that can achieve the highest reduction in GHG emissions is to capture carbon dioxide from the conventional power generations. The electricity power plants are commonly represented as the largest source of CO2 amongst other commercial industries [3]. Therefore, the existing power plants have to be precisely investigated in order to overcome the extra cost of switching to CO_2 capture plants and to improve their performance at similar operating conditions to those of non- CO_2 capture plants.

Several techniques to capture carbon dioxide are being increasingly developed. The three main techniques that are developed for the capture of CO_2 are pre-combustion capture, post-combustion capture, and oxy-fuel combustion. Oxy-fuel combustion technology has been widely considered as a viable option to control and reduce several types of gaseous emissions from PC power plants [1]. The oxy-fuel combustion is to burn fossil fuel with pure oxygen (produced in cryogenic air separation units) and recycled flue gas (RFG) to produce a high concentration of CO_2 in the flue gas. This technique will lead to make its separation and compression processes easier and more cost-effective.

Using pure oxygen and RFG instead of air to burn fuel was firstly used by Abraham [4]. The purpose was to increase CO_2 concentrations, which can be economically used for enhanced oil recovery by injecting CO_2 underground for permanent storage. In the last few years, many comparisons have been experimentally conducted on the solid fuel combustion in air and in mixtures of O_2/ CO_2 [5-7]. Oxygen concentrations in feed gas, heat transfer and flame characteristics in oxy-fuel combustion should be precisely studied to achieve similar combustion characteristics to the conventional combustion case.

The numerical calculation methods can extensively

provide a wide range of efficient information in furnace and burner's design before making any expensive and time-consuming experimental studies. To our knowledge, there is still little research work conducted on the oxy-fuel combustion in numerical modelling. Therefore, this study is focused on the numerical solution to give a good insight in the physical and chemical mechanisms of oxy-fuel combustion technique. In the present study, temperature distributions, species concentrations, and velocity components are numerically calculated under air-fired and oxy-fuel combustion environments for a 100 kW down-fired furnace. Therefore, the purpose of this work is to validate the CFD model, and to compare the above-mentioned variables for both the combustion cases. The same volumetric flow rates of fuel (propane) and reactants (O_2/N_2) or (O_2/CO_2) are used in feed gases based on the measurements set up.

2. MATHEMATICAL MODELS

The commercial CFD, AVL Fire ver.2008.2 code is employed to analyze the computational domain system that includes chemical reaction, radiative heat transfer, fluid flow field, and turbulent models. It is important to accurately calculate and predict the temperature levels, turbulent flow fields, and species concentrations from combustion systems. In order to illustrate the applications of CFD on the turbulent non-premixed gaseous combustion, it is necessary to define all the mathematical models associated with combustion phenomenon.

2.1. Flow Field Model

To illustrate the turbulent non-premixed flame characteristics of propane (C_3H_8) combustion in air and O_2/CO_2 mixture, the three-dimensional governing equations of mass conservation, momentum, and energy transport equations in the transient conditions have been solved in the Cartesian tensor form:

Mass conservation equation

$$\frac{\partial \rho}{\partial t}+\frac{\partial}{\partial x_i}(\rho u_i)=0 \tag{1}$$

-

Momentum conservation equation

$$\frac{\partial}{\partial t}(\rho u_i)+\frac{\partial}{\partial x_j}(\rho u_i u_j)=-\frac{\partial P}{\partial x_i}+\frac{\partial}{\partial x_j}(\tau_{ij})_{eff}+\frac{\partial}{\partial x_j}\left(-\overline{\rho u_i' u_j'}\right) \tag{2}$$

-Energy transport equation

$$\frac{\partial}{\partial t}(\rho E)+\frac{\partial}{\partial x_i}[u_i(\rho E+P)]=\frac{\partial}{\partial x_j}\left(k_{eff}\frac{\partial T}{\partial x_j}+u_i(\tau_{ij})\right)+S_\phi \tag{3}$$

where ϕ denotes enthalpy and concentration of species, while term S_ϕ represents the appropriate source of the variables ϕ. The local density of the mixture is dependent on pressure, reactants, products concentrations, and temperature and determined through the equation of state:

$$\rho=\frac{P}{RT\sum_k^{sp}\frac{Y_k}{(MW)_k}} \tag{4}$$

While the temperature values can be calculated from the enthalpy:

$$T=\frac{h-\sum_k^{sp}Y_k\Delta h_{fu}}{\overline{c_p}} \tag{5}$$

The effective stress tensor and thermal conductivity are given by:

$$(\tau_{ij})_{eff}=\mu_{eff}\left(\frac{\partial u_j}{\partial x_i}+\frac{\partial u_i}{\partial x_j}\right)-\frac{2}{3}\mu_{eff}\frac{\partial u_i}{\partial x_i}\delta_{ij} \tag{6}$$

$$K_{eff}=K+\frac{c_p\mu_t}{\sigma_t} \tag{7}$$

Fuel and feed oxidizer gases (air or O_2/ CO_2) are non-premixed before entering into the furnace according to the burner's design. In this numerical study, it is assumed that the swirl created by the primary and secondary registers. This can ensure better mixing conditions for reactants in order to avoid any external recirculation in the flame structure and to keep it in stable form during burning reactants.

2.2. Species Transport Model

In order to reduce the number of equations to be solved, dimensional quantities are introduced to express the reactive system. The mass fraction, residual gas mass fraction, and mixture fraction are given by [8]:

$$y_{fu}=\frac{m_{fu,u}}{m_{tot}} \tag{8}$$

$$g=\frac{m_{rg}}{m_{oxid}} \tag{9}$$

$$f=\frac{m_{fu,u}+m_{fu,b}}{m_{tot}} \tag{10}$$

The solution of transport equations for the density weighted mean quantities y_{fu}, f, and g is illustrated in the following equations:

$$\frac{\partial}{\partial t}(\rho y_{fu})+\frac{\partial}{\partial x_i}(\rho U_i y_{fu})=\frac{\partial}{\partial x_i}\left(\Gamma_{fu}\frac{\partial y_{fu}}{\partial x_i}\right)+S_{fu} \tag{11}$$

Where $S_{fu}=\rho.\dot{r}_{fu}$, this term will briefly explain in the combustion model section.

$$\frac{\partial}{\partial t}(\rho f)+\frac{\partial}{\partial x_i}(\rho U_i f)=\frac{\partial}{\partial x_i}\left(\Gamma_f\frac{\partial f}{\partial x_i}\right) \tag{12}$$

$$\frac{\partial}{\partial t}(\rho g)+\frac{\partial}{\partial x_i}(\rho U_i g)=\frac{\partial}{\partial x_i}\left(\Gamma_g\frac{\partial g}{\partial x_i}\right) \tag{13}$$

The chemical reaction system in this study consists of five species: C_3H_8, O_2, CO_2, H_2O, and N_2. With the following algebraic expressions, the mass fraction of the above-mentioned species can be calculated in terms of

the total mixture mass:

$$\left.\begin{aligned} y_{o_2} &= a_1\left[(1-f)-S\left(f-y_{fu}\right)\right] \\ y_{N_2} &= (1-a_1)(1-f) \\ y_{pr} &= 1-y_{fu}-y_{o_2}-y_{N_2} \\ y_{co_2} &= a_2 y_{pr} \\ y_{H_2O} &= a_3 y_{pr} \end{aligned}\right\} \qquad (14)$$

The parameters a_i are the mass fractions of ith species: O_2, CO_2, and H_2O, S is stoichiometric air/ fuel ratio, while n and m are representing the number of carbon and hydrogen atoms in the hydrocarbon fuel (C_nH_m =C_3H_8).

2.3. Combustion Model

The numerical simulation of the mean chemical reaction rates considers a main problem in the determination of chemical kinetic processes. This complicated calculation is due to non-linear functions of the local values of temperature and species concentrations. A single step irreversible reaction of a hydrocarbon fuel (C_3H_8) with air or O_2/CO_2 mixture is considered in this study. According to the experimental operating conditions of this gaseous combustion, the chemical reaction equations were with 15% excess air:

Air-fired combustion chemical equation

$$C_3H_8+5.75(O_2+3.76N_2)\rightarrow 3CO_2+4H_2O+0.75O_2+21.62N_2 \qquad (15)$$

-Oxy-fuel fired combustion chemical equation

$$C_3H_8+5.75O_2\rightarrow 3CO_2+4H_2O+0.75O_2 \qquad (16)$$

Turbulence controlled combustion model, Eddy Breakup (EBU) model, is used for these combustion simulations. The EBU model is a popular and an efficient model in combustion calculation, which was firstly proposed by Spalding [9] and modified later by Magnussen and Hjertager [10].

The mean reaction rate can be written according to [10]:

$$\overline{\dot{\rho r}}_{fu}=\frac{C_{fu}}{\tau_R}\overline{\rho}\min\left(\overline{y}_{fu},\frac{\overline{y}_{Ox}}{S},\frac{C_{pr}\,\overline{y}_{pr}}{1+S}\right) \qquad (17)$$

The rate of consumption of fuel is specified as a function of local flow properties, thus it is dependent upon the turbulent time scale (τ_R). The first two terms of the minimum value of operator simply verify if fuel or oxygen is present in limiting quantity, and the third term is used for a reaction possibility. C_{fu} and C_{pr} are empirical coefficients, and the exact values for these coefficients are dependent on the fuel and the detailed structure of the turbulent flow field. More than twenty simulation tests were carried out to adjust and select the perfect values according to available experimental data [11]. The best results found out that by increasing the values of these coefficients lead to an intensification of the turbulent reaction rate. Therefore, under these special conditions of this study, C_{fu} and C_{pr} are set to 6.0 and 0.5 for air-fired case, and 3.0 and 0.5 for oxy-fuel fired. Detailed information related to the mathematical models and computational method descriptions used in this study can be found in the previous preliminary CFD study [12].

3. BOUNDARY CONDITIONS AND MESH

The inlets of fuel and other oxidizers in primary and secondary registers are located in the central position of the top-wall of furnace. The initialization information is kept constant for both combustion cases such as an initial temperature (298.15 K) and initial pressure (101325 Pa). The velocities of primary and secondary registers of oxidizers (air or O_2/CO_2) are affected by the fin angles 45^0 (normal velocity V_n = 8.46 m/s) and 15^0 (normal velocity V_n = 3.32 m/s), respectively in order to stabilize the flame structure of combustion.

For precise modelling, the wall of furnace is divided into two parts: top-wall and vertical-wall. For both parts of wall, no-slip condition (u, v, and w = 0) and wall emissivity (ε = 0.41 for air-fired case and ε = 0.52 for oxy-fuel firing case) are applied, but the temperature value was only constant for top-wall (925 K) and changeable for vertical-wall. Two second-degree polynomial functions are used to calculate the temperature distribution along the vertical-wall in order to match the real values of experimental data in that region of the furnace wall.

A higher mesh concentration is used along the centerline axis of furnace, while the mesh size is gradually increased away nearby the wall and outlet boundaries as shown in Fig.1.

Three different non-uniform structured grid systems are used for grid independence test with 224000, 480000, and 595200 cells. The grid independence test indicated that the grid number (480000) satisfies more accurate results amongst the other grid systems. It made a good balance between the computational accuracy and the computing cost.

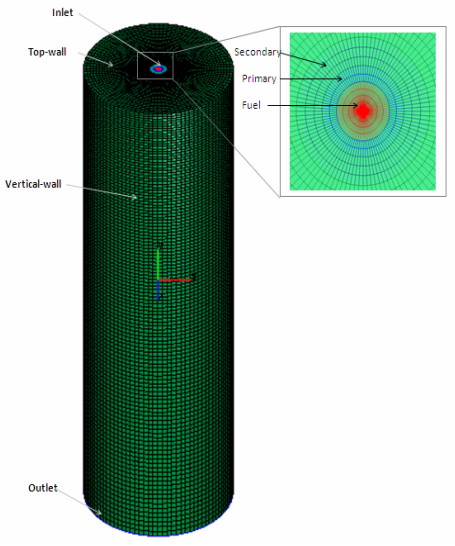

Fig 1. Grid system of computational domain

4. RESULTS AND DISCUSSION

The composition of feed gases for both primary and secondary registers of oxy-fuel combustion case was composed of 21% vol. of O_2 (similar to that of air-fired case) and 79% vol. of CO_2. This change in combustion media led to a significant impact on the combustion characteristics and flame structure. Fig. 2 shows temperature distributions of air-fired flame and oxy-fuel flame at the vertical cut of the furnace. The air-fired flame exhibits a more bright aspect than the oxy-fuel flame. This feature of flame luminous appearance can highly be attributed to the capability of CO_2 to absorb radiation in the latter flame, which has the higher concentration in the flue gas compared to air-fired case. On the other hand, the oxy-fuel flame, which has the same oxygen concentration in the feed gases, showed that the flame was obviously concentrated in the central position, and it was not spread inside the furnace compared to the air-fired flame.

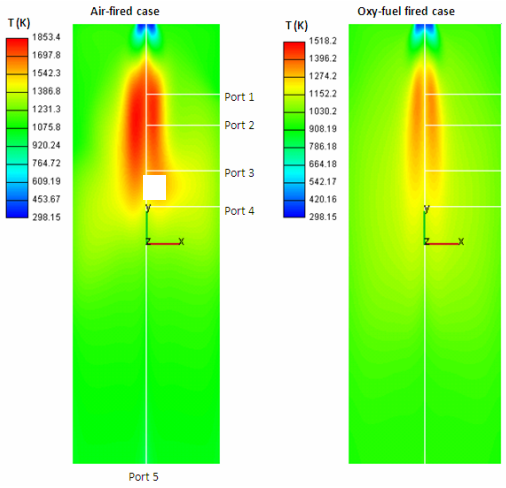

Fig 2. Temperature distributions (K) for the air-fired flame (left) and the oxy-fuel flame (right) at the vertical cut (X - Y plane) of furnace.

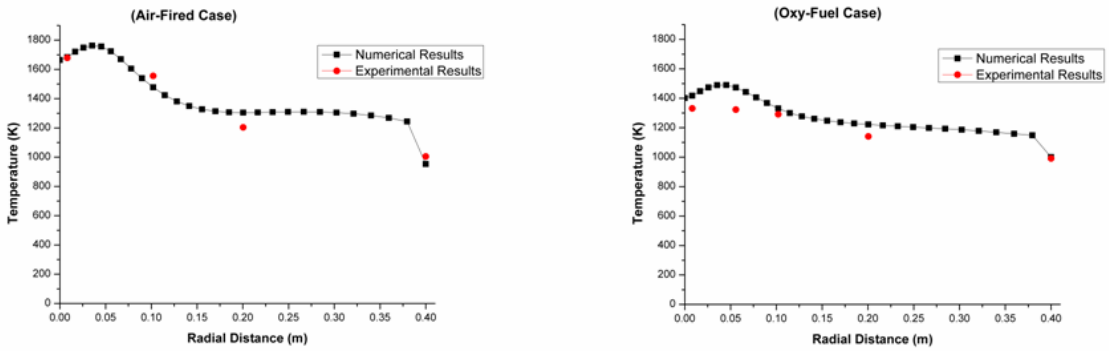

Fig 3. Temperature distribution at 553 mm from burner exit for air-fired and oxy-fuel combustion cases.

In addition, the peak flame temperature level of combustion was drastically decreased from 1853 K for the air-fired case to 1518 k for the oxy-fuel case. This drop in the flame temperature is significantly affected the combustion delay in oxy-fuel case. These numerical results of combustion delay in the oxy-flame were extremely consistent with the recent study of Ref. [13].

However, these differences in the flame shapes between air-fired flame and oxy-fuel fired flame are principally due to the differences in the thermodynamics properties between nitrogen and carbon dioxide, and radiative properties of gas mixture.

Fig. 3 illustrates the validation and comparison of the temperature profiles at 553 mm from burner exit plane for the air-fired and the oxy-fuel combustion cases. The overall agreement was achieved in this challenging location except for oxy-fuel case. Peak temperature was occurred between central point of the furnace and 0.1 m in the radial direction. This can be firstly explained due to the intensive region of combustible gases; secondly because of the concentration of flame in this radial distance of the furnace that led to a slight increase in the flame temperature level. These numerical results revealed that the mixture fractions were closer to Stoichiometric (theoretical $\xi = \xi_{ST}$) characteristics. This means that the entire oxygen and fuel were completely consumed, and as a result the flame temperature was at a maximum value.

Fig. 4 shows the velocity vectors of the primary and secondary swirl registers of the burner at the inlet of the furnace. This swirl ensures that the fuel is completely burnt in the closest region to the burner exit, and therefore eliminates undesirable gases such as carbon monoxide (CO), smoke, soot, etc. In Fig. 5, the effect of swirl numbers (S) on the stability of flame in three different recirculation zones is showed. The recirculation zones of the flow field were divided into three different separate zones: internal recirculation zone, reaction zone, and external recirculation zone. The swirl numbers were 0.79 and 0.21 for the primary and secondary registers, respectively. These swirls are used to enhance mixing zone between the fuel and oxidizer (air or O_2/CO_2) streams. Due to this swirl effect, well-mixing conditions were achieved in the closest region to the burner exit, and

therefore it might avoid the gases travel downstream of the furnace to a well-mixing point. In addition to the well-mixing conditions, the aerodynamic effect of swirl can shorten the flame length.

At the most intense combustion location (port 1), Fig. 6 shows a comparison between the experimental data and the predicted results for the mass fraction distribution of carbon dioxide for both combustion cases in wet basis.

For the air-fired case, over-prediction was noticed; while the oxy-fuel case showed relatively better predictions except from the central point of the furnace to ~0.08 m in the radial direction. However, this location of the furnace is obviously showed increasing carbon dioxide concentrations for the oxy-fuel combustion case.

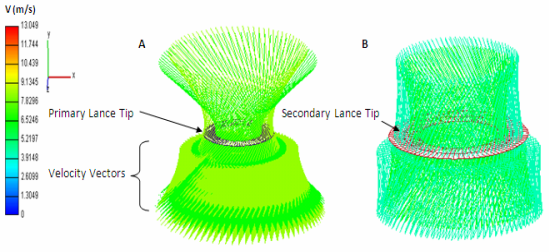

Fig 4. Velocity vectors (m/sec) of primary (A) and secondary (B) swirl registers at the burner exit plane.

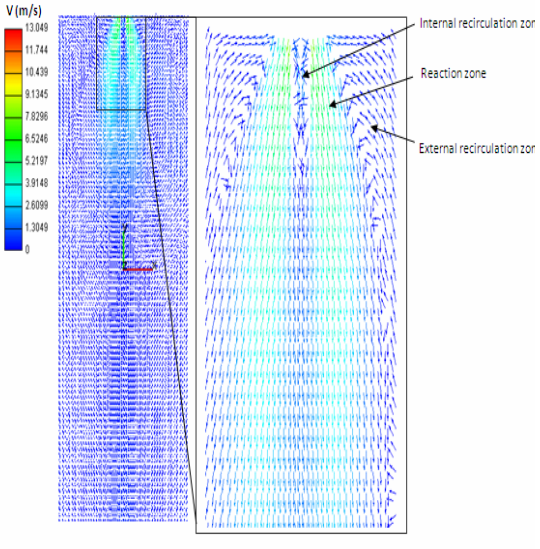

Fig 5. Inlet velocity vectors (m/sec) of three different recirculation zones.

As the nitrogen is replaced by CO_2 in the feed gases, carbon dioxide concentration is highly increased from around 15 % (kg/kg) to 76 % (kg/kg) under wet basis in flue gas. This result reveals that the carbon dioxide concentration was increased by approximately 5 times in wet basis.

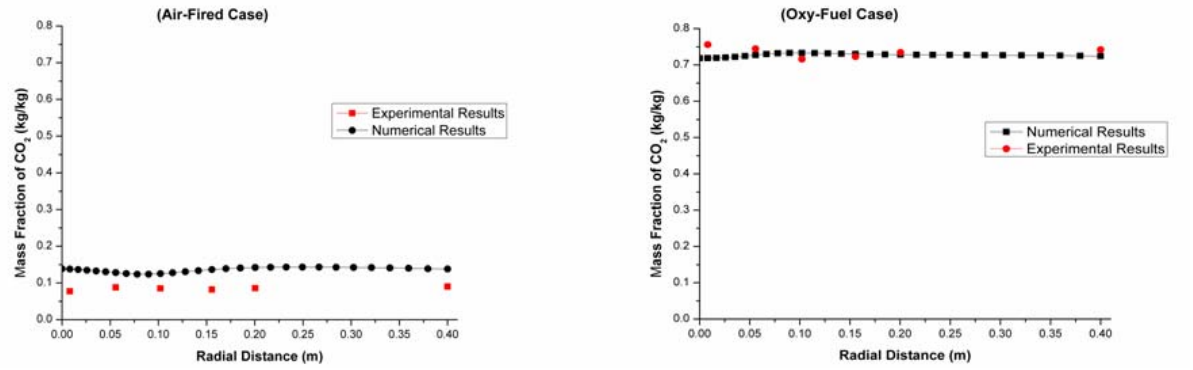

Fig 6. Mass fraction distribution of carbon dioxide at 384 (mm) from burner exit plane for the air-fired and the oxy-fuel combustion cases in wet basis.

5. SUMMARY AND CONCLUSIONS

A three-dimensional Computational Fluid Dynamics (CFD) model has been developed to simulate the air-fired and oxy-fuel combustion cases. The temperature distribution levels, species concentration, and velocity distributions were investigated at the most intense combustion locations of the furnace. An efficient combustion model (EBU) with the most appropriate empirical coefficients is used in this study. Primary and secondary swirl registers are employed to enhance an internal recirculation mechanism of flames and to ensure a well-mixing condition for turbulent non-premixed gaseous reactants.

Slight over-predictions of temperature levels and species concentration levels are noticed compared to the measurements. These over-predict may be occurred because of neglecting the multi-step chemical reactions, which lead to dissociate carbon dioxide and water vapour in the combustible products into several intermediate species. The numerical results showed that the flame is clearly concentrated in the central position in oxy-fuel case, and it is not spread inside the furnace compared to the air-fired flame. The combustion delay in oxy-fuel case is evident. This delay is likely happened due to insufficient oxygen consumption at the near-burner region compared to the reference case. The residence time of combustible reactants is considerably increased due to adopting the swirl injection system that leads to enhance flame stability. The carbon dioxide concentration rises up by ~ 5 times for oxy-fuel compared to air-fired case under wet basis.

Finally, even though there are some discrepancies between the measured data and numerical results, the CFD results are considerably showed the same qualitative trend as the experiments. However, this study represents the second stage of the entire simulation of oxy-fuel combustion. The next step of this project will comprehensively focus on the brown coal combustion in the full-scale tangentially-fired furnace under oxy-fuel combustion technique.

6. ACKNOWLEDGEMENTS

The authors wish to thank the ministry of higher education and scientific research (MOHESR) in Iraqi Government for the financial support during the scholarship period (2009-2012) in Australia.

7. REFERENCES

1. T. Wall, Y. Liu, C. Spero, L. Elliott, S. Khare, R. Rathnam, F. Zeenathal, B. Moghtaderi, B. Buhre, C. Sheng, R. Gupta, T. Yamada, K. Makino, J. Yu, 2009, “An overview on oxyfuel coal combustion--State of the art research and technology development”, Chemical Engineering Research and Design, 87 1003-1016.
2. J. Davison, 2007, “Performance and costs of power plants with capture and storage of CO_2”, Energy, 32 1163-1176.
3. H. Liu, R. Zailani, B.M. Gibbs, 2005, “Comparisons of pulverized coal combustion in air and in mixtures of O_2/CO_2”, Fuel, 84, 833-840.
4. B.M. Abraham, 1982, “Coal-oxygen process provides CO_2 for enhanced recovery”, Oil Gas J.; (United States); Journal Volume: 80:11, Pages: 68-70, 75.
5. H. Liu, R. Zailani, B.M. Gibbs, 2005, “Comparisons of pulverized coal combustion in air and in mixtures of O 2/CO2”, Fuel, 84 , 833-840.
6. Y. Tan, E. Croiset, M.A. Douglas, K.V. Thambimuthu, 2006, “Combustion characteristics of coal in a mixture of oxygen and recycled flue gas”, Fuel, 85, 507-512.
7. T. Suda, K. Masuko, J. Sato, A. Yamamoto, K. Okazaki, 2007, “Effect of carbon dioxide on flame propagation of pulverized coal clouds in CO_2/O_2 combustion”, Fuel, 86, 2008-2015.
8. Anonymous: 2008, AVL Fire CFD Solver v 8.5 manual, A-8020 Gras, Austria, www.avl.com.
9. D.B. Spalding, 1971, “Mixing and chemical reaction in steady confined turbulent flames”, Symposium (International) on Combustion, 13 649-657.
10. B.F. Magnussen, B.H. Hjertager, 1977, “On mathematical modeling of turbulent combustion with special emphasis on soot formation and combustion”, Symposium (International) on Combustion, 16, 719-729.
11. K. Andersson, 2007, “Characterization of oxy-fuel flames - their composition, temperature and radiation”, Chalmers University of Technology, Thesis, Göteborg.
12. A. H. Al-Abbas, J. Naser, D. Dodds, 2011, “CFD modelling of air-fired and oxy-fuel combustion of lignite in a 100 kW furnace”, Fuel, 90, 1778-1795.
13. J. D. Moore and K. K. Kuo, 2008, “Effect of switching methane/oxygen reactants in a coaxial injector on the stability of non-premixed flame”, Combustion Science and Technology, 180, 401-417.

8. MAILING ADRESS

Jamal Naser
Faculty of Engineering and Industrial Science,
Swinburne University of Technology,
Hawthorn, Victoria 3122,
Australia.